applied sciences

MDPI

Article

Plasma Enhanced Wet Chemical Surface Activation of TiO_2 for the Synthesis of High Performance Photocatalytic Au/TiO_2 Nanocomposites

Nguyen Thi Thu Thuy [1,2], Do Hoang Tung [3,*], Le Hong Manh [3], Joon Heon Kim [4], Sergey Ivanovich Kudryashov [5], Pham Hong Minh [3] and Nguyen The Hien [1]

1 Faculty of Engineering Physics and Nanotechnology, VNU University of Engineering and Technology, 144 Xuan Thuy Road, Cau Giay District, Hanoi 10000, Vietnam; thuthuyt34@gmail.com (N.T.T.T.); ngoduonghoaianh@gmaill.com (N.T.H.)
2 Department of Fundamental of Fire Fighting and Prevention, University of Fire Prevention and Fighting, 243 Khuat Duy Tien, Thanh Xuân, Hanoi 10000, Vietnam
3 Institute of Physics, Vietnam Academy of Science and Technology, Vietnam, 18 Hoang Quoc Viet Street, Cau Giay District, Hanoi 10000, Vietnam; lehongmanh@gmail.com (L.H.M.); lhthu.cgd@maill.com (P.H.M.)
4 Biomedical and Nanophotonics Laboratory, Advanced Photonics Research Institute, GIST, Gwangju 61005, Korea; joonhkim@gist.ac.kr
5 Lebedev Physical Institute, Leninskiy Prospect 53, Moscow 119991, Russia; sikudr@sci.lebedev.ru
* Correspondence: dhtung@iop.vast.ac.vn

Received: 7 April 2020; Accepted: 8 May 2020; Published: 12 May 2020

Abstract: To enhance the effectiveness of TiO_2 as a photocatalyst, it was believed that the drawbacks of the large bandgap and the rapid electron-hole recombination can be overcome by coupling TiO_2 with plasmonic metal nanoparticles. The incorporation of the nanoparticles onto the TiO_2 surface requires a suitable procedure to achieve the proper particle adhesion. In this work, we propose a simple, clean, and effective surface activation of TiO_2 using plasma enhanced wet chemical surface treatment. Under only 5 min of plasma treatment in a 3% NH_3/3% H_2O_2 solution, gold nanoparticles were found better adhered onto the TiO_2 surface. Hence, the methylene blue degradation rate of the Au/TiO_2 under sunlight treated was improved by a factor of 3.25 times in comparison to non-treated Au/TiO_2 and by 13 times in comparison to the bare rutile TiO_2.

Keywords: plasma-liquid interaction; sunlight degradation; Au/TiO_2 nanocomposite; surface treatment; noble metal based photocatalyst

1. Introduction

Titanium dioxide (TiO_2) is regarded as one of the most fascinating materials for environmental applications [1,2]. It has been intensively investigated as a photocatalyst due to its high photocatalytic activity. Despite numerous advantages, such as low fabrication cost, environmental friendliness, and high chemical stability, TiO_2 still cannot be widely applied due to its inherent drawbacks. TiO_2 has a rapid electron-hole recombination [3] and a high bandgap energy [4]. These drawbacks can be overcome by coupling the semiconductor with plasmonic metal nanoparticles [5]. The plasmonic metal nanoparticles are expected to not only improve the visible light absorption, but also to minimize the electron-hole recombination reaction in TiO_2. It has been demonstrated that surfacial plasmonic resonance improved the light absorption, increased the charge separation, and enhanced the suppression of electrons and holes, and thus significantly improved hydrogen generation [6].

There are many methods to support the adhesion of Au nanoparticles on the titania surface, such as photodeposition [7], deposition–precipitation [8], as well as the sol–gel method [9,10]. However,

the improvement of the photocatalyst activity (PCA) in Au loaded titania is just several times higher than that of the original one. This may be due to the week connection between the Au nanoparticles and the TiO_2 surface. It is noted that PCA shows significantly more improvement in the one spot synthesis method than in the multistep one [9].

In order to improve the adhesion of gold nanoparticles on its surface, TiO_2 normally follows a lengthy complicated procedure of surface activation to attach the oxygenic or nitrogenous functional groups or even both on its surface and subsequently undergoes a surface functionalization by adding the appropriate ligands (e.g., MPTMS–3-mercapto-propyl-tri-metoxy-silane). For example, Rehacek et al. [11] used a solution of NH_4OH:H_2O_2:H_2O (5:1:1 in volume) to treat TiO_2 for 20 h at room temperature or under the UV radiation for 1 h and then illuminated with deep ultraviolet (DUV) for 10 min to improve its wettability. Higgins et al. [12], however, incubated TiO_2 at 80 °C in a NaOH solution for 1 h to add the OH groups and then in a urea solution for 4 h to add the nitrogenous groups.

Plasma technology has been efficiently used in the fabrication of nanomaterials [13] especially the plasma–liquid interaction method [14]. For gold nanoparticle synthesis, Au^{3+} can be reduced either by solvated electrons or by reactive species generated in the solution [15]. The two most dominant reactions are:

$$[AuCl_4]^+ + 3e^-_{aq} \rightarrow Au^0 + 4Cl^-$$

and

$$nH_2O_2 + nOH + Au^{3+} \rightarrow [AuCl_4]^+ + nHO_2^- + nH_2O$$

where e^-_{aq} stands for solvated electron.

Recently, the electrochemical reduction of $HAuCl_4$ acid in dense hydrosols of high-index diamond sub-micrometer sized particles was tested as a promising "green" fabrication route for "metallic nanoparticle–dielectric" clusters in their colloidal solutions. The plasma–liquid interaction approach requires only water-based solutions with the metal precursor and is completely free of any additional reducing and/or capping agents [16]. It showed successful decoration of gold nanoparticles (AuNPs) onto the diamond surface. In the presence of the diamond particles, substantial "red" spectral shifts of the plasmonic resonance were observed for the AuNPs, being more pronounced for the decorated diamond particles (≈536 nm), than for those adsorbed AuNPs on their surfaces from the mechanical mixture of their colloids (≈530 nm). These shifts of the plasmonic resonance peak could be unambiguously related to the high-index dielectric environment of the AuNPs, provided by their attachment to the diamonds [17].

Many studies on nonequilibrium gas phase plasmas–fluid interactions have been performed. In particular, the reactive transient species in the interfacial plasma–fluid region play a critical role in plasma-induced liquid reactivity [18,19]. Moreover, the reactants are activated by the plasma or the heat produced by the plasma and, in some cases, the liquid can also act as a moderator suppressing or delivering plasma processes with excess energy.

In this work we propose a novel, simple, clean, and effective surface activation of TiO_2 using the plasma enhanced wet chemical surface treatment. Plasma–liquid interaction speeds up the surface treatment of TiO_2 with NH_3/H_2O_2 solution for the better attachment of the Au nanoparticles. This treatment helps minimize the need of NH_3 and H_2O_2 as well as the treatment time, but still improves the PCA of the Au/TiO_2 nanocomposites.

2. Materials and Methods

Commercial submicron (averaged size ca. 800 nm) rutile TiO_2 particles (R800) from US Research Nanomaterials, Inc. Houston, TX 77084, United States, were used in our studies. Au(III) chloride trihydrate (99.9%; $HAuCl_43H_2O$) was purchased from Sigma–Aldrich, while 30% hydrogen peroxide solution and 25–28% ammonia solution were purchased from Xilong Scientific Co., Ltd, Chaoshan Road, Shantou, Guangdong 510663, China.

The micro-plasma system consisted of a DC high voltage source, a plasma nozzle, a gold electrode and a 50 mL glass beaker from Bomex with 20 mL treatment solution (see Figure 1). The plasma nozzle had a Teflon housing with one end being a hollow cylinder of 15 mm in outer diameter and 10 mm in inner diameter, covering the plasma electrode, and the other end being connected to a 6 mm quick gas connector. In our experiments, the plasma electrode was a sharpened 1.6 mm diameter tungsten rod connected to the high voltage via a 100 kΩ resistor. The other polarity was grounded and connected to the gold electrode, which was submerged into the solution. The processing current was maintained constantly at 5 mA.

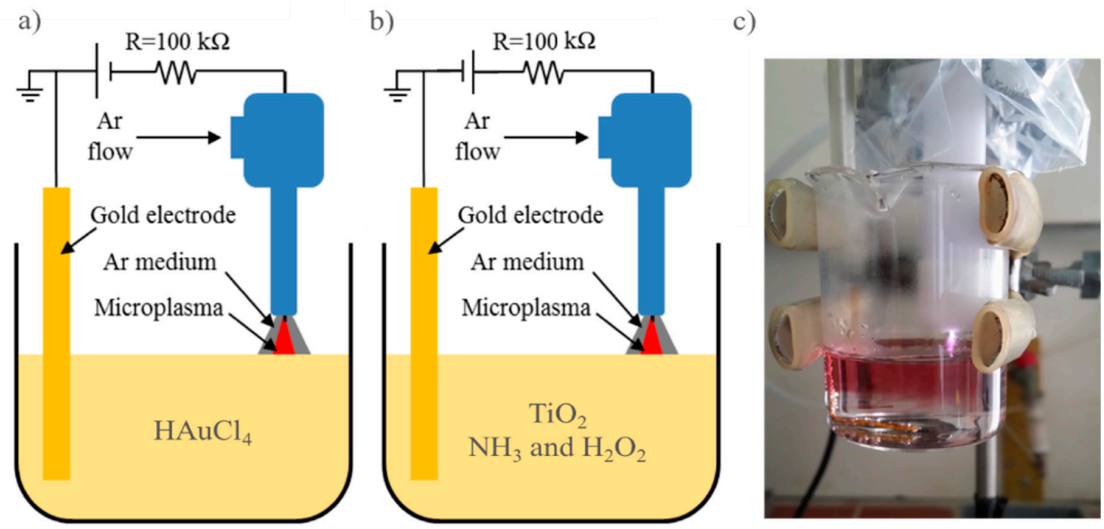

Figure 1. Micro-discharge workstation for (**a**) the electrochemical gold reduction, (**b**) the TiO_2 treatment and (**c**) image of running plasma for gold nanoparticle synthesis from $HAuCl_4$ 0.06 mM precursor solution.

In order to synthesize gold nanoparticles (AuNPs) from $HAuCl_4$ solution, we use the above mentioned plasma system with the negative polarity of the plasma electrode (Figure 1a). Several precursor concentrations were used to study the gold nanoparticle productivity of the system.

The schematic synthesis and diagnostic procedures of Au/TiO_2 composites are presented in Figure 2. In order to prepare the treated TiO_2 samples, 20 mL TiO_2 0.1 g·L^{-1}, 3% NH_3, and 3% H_2O_2 were first subjected to a positive plasma (Figure 1b) for 5 min to modify the TiO_2 surface. After that, 0.12 mL $HAuCl_4$ 10 mM was added together with 0.25 mL DI water to get 20 mL solution of treated TiO_2 0.1 g·L^{-1} and $HAuCl_4$ 0.06 mM (about 0.37 mL water was vaporized under the plasma treatment). Non-treated TiO_2 samples were prepared by simply adding NH_3, H_2O_2, and $HAuCl_4$ solutions to get 20 mL TiO_2 0.1 g·L^{-1}, 3% NH_3, 3% H_2O_2, and 0.06 mM $HAuCl_4$.

Both treated and non-treated TiO_2 were then irradiated with the negative plasma (configuration in Figure 1a) for 15 min to completely reduce Au(III) to form the desired Au/TiO_2 nanocomposites. The resulting solutions were subsequently vacuum dried to eliminate all remaining H_2O_2 and NH_3. Suppose all Au precursor has been reduced to AuNPs, one can easily calculate that the gold particles loaded on the TiO_2 in these Au/TiO_2 nanocomposite samples is of about 11.8% in weight. 10 mL DI water was added to the samples to get 10 mL 0.2236 g·L^{-1} Au/TiO_2, treated and non-treated samples.

To investigate and compare the sunlight photocatalyst activity of and among the bare TiO_2, the non-treated and treated Au/TiO_2, using above sample preparation procedure we fabricated in darkness 2 mL solution of treated Au/TiO_2 0.1118 g·L^{-1} and Methylene blue (MB) 20 mg·L^{-1}; 2 mL solution of non-treated Au/TiO_2 0.1118 g·L^{-1} and MB 20 mg·L^{-1}; and 2 mL solution of 0.1 g·L^{-1} bare TiO_2, MB 20 mg·L^{-1}.

The decomposition of MB under the solar simulator irradiation (AM 1.5) with a power of 100 mW cm^2 (Oriel SollA) was analyzed by following the evolution of its characteristic absorbance

peak at 664 nm. The time dependent concentrations of MB obtained through the experiments were fitted to pseudo-first order kinetics as follows:

$$ln\left(\frac{C_t}{C_0}\right) = -k \cdot t$$

where Co ($g \cdot L^{-1}$) and Ct ($g \cdot L^{-1}$) are the concentrations of MB before irradiation and at a given time t (in minute-min), respectively; k is the pseudo-first order rate constant (min^{-1}).

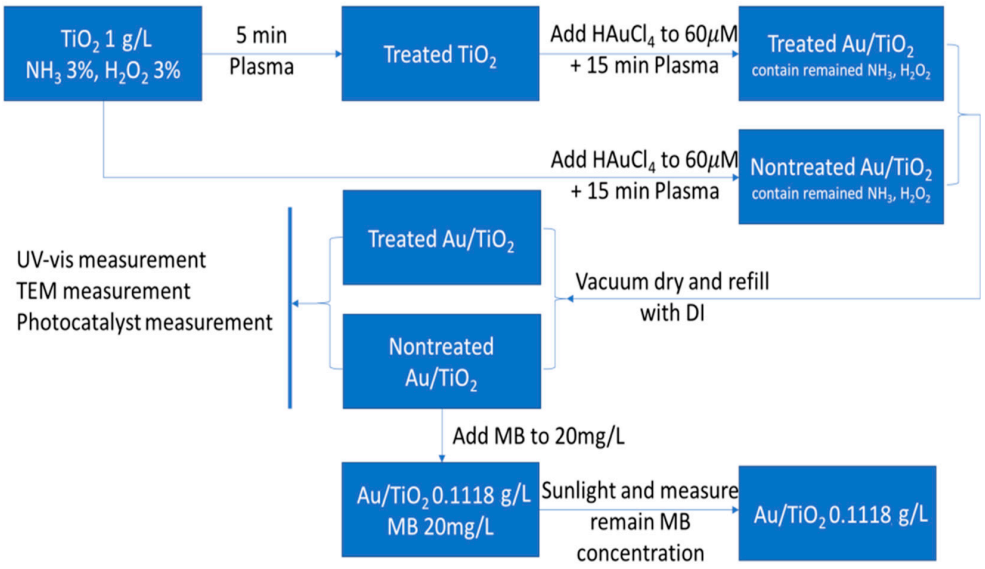

Figure 2. Schematic synthesis and diagnostic procedures of Au/TiO_2 composites.

The UV-vis absorbance of the aqueous samples in a 1 cm wide quartz cuvette was measured with an UV-near IR spectrometer of the type V-570 (Jasco). The particle morphologies were examined in a transmission electron microscope (TEM) JEM 1010.

3. Results and Discussion

In order to investigate the activating ability of plasma on the solution, we compared the decolorization of methylene blue (MB) with three solutions; 20 mL 10% hydroperoxide, 20 mL 10% hydroperoxide treated with 5 min of plasma (plasma activated H_2O_2), and 20 mL deionized water treated with 5 min of plasma (plasma activated DI). UV-vis absorption spectroscopy was used to trace the time evolvement of 665 nm absorption peak after 1 mL solution of MB 40 $mg \cdot L^{-1}$ was added into these solutions (see Figure 3). The MB concentration gradually decreased in the untreated H_2O_2. In contrast, it showed a small drop of about 2% in plasma activated DI then remained unchanged. However, in plasma activated H_2O_2, the concentration showed a stepwise evolution with a large drop of about 17% then followed by a gradual decrease with larger slop in comparison to the untreated H_2O_2.

The concentration drops in the plasma treated solutions were attributed to the transient reactive species created by plasma which react very fast with MB. This result confirms the activating ability of plasma on reactant solutions. With the presence of H_2O_2 in the liquid, plasma can create significant amount of transient reactive species, making the plasma treated solution become more reactive.

In order to find out the optimal conditions for the gold nanoparticle synthesis using our plasma–liquid interaction system [16], different precursor concentrations were used and treated with negative plasma for 15 min and the absorption spectra of the as-obtained solutions were checked. As can be seen in Figure 4, the UV-vis absorption spectra of the as-obtained solutions show the characteristic absorption peaks of the gold nanoparticles. The position and the intensity of the absorption peaks significantly depend on the precursor concentration. When the precursor

concentration increases from 0.015 mM to 0.12 mM, the absorption peak position shifts up from ca. 528 nm to ca. 558 nm, while the peak intensity first increases sharply with precursor concentration, reaches its maximum with $HAuCl_4$ concentration of 0.06 mM then gradually drecreases. For this investigation, therefore, we used 0.06 mM $HAuCl_4$ as an optimal precursor to generate AuNPs for the synthesis of Au/TiO_2 nanocomposites. At this precursor concentration, the plasma–liquid interaction creates fairly uniform spherical AuNPs with the size in the range of about 35–45 nm (see Figure 4) and the characteristic absorption peak at about 534 nm.

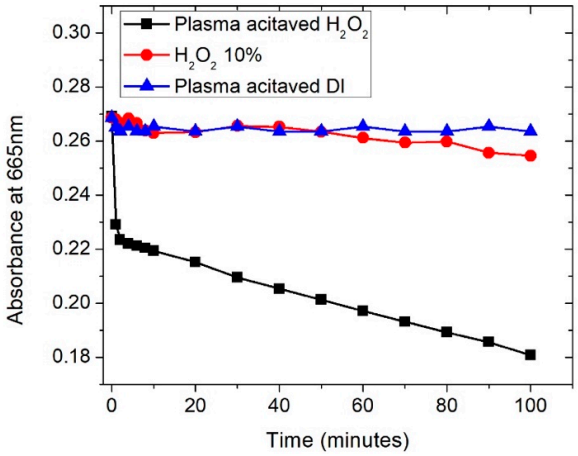

Figure 3. Time evolution of absorption peak at 665 nm of methylene blue after being added to plasma activated 10% H_2O_2, 10% H_2O_2, and plasma activated deionized water solutions.

Gold nanoparticles were also generated at the 0.06 mM precursor concentration with another plasma–liquid interaction configuration as reported in [20]. The authors there have attained smaller particle sizes distributed around about 20 nm, but the characteristic absorption peak was positioned at about 534 nm like in our case. The reason for the discrepancy in the particle size may be attributed to the shape of the obtained AuNPs. As reported in [9], AuNPs were obtained in quite diverse shapes including spherical, triangular, cubic, hexagonal, and pentagonal grains and also bars, whereas in our experiments the AuNPs were mostly in the spherical shape with rather uniform size (see Figure 5). In their setup, the authors used a hollow electrode type so the plasma channel was surrounded by air. Meanwhile, in our case, the rod electrode was surrounded by the Ar medium. This difference in the plasma medium may be attributed to the difference in the Ar nanoparticle shapes.

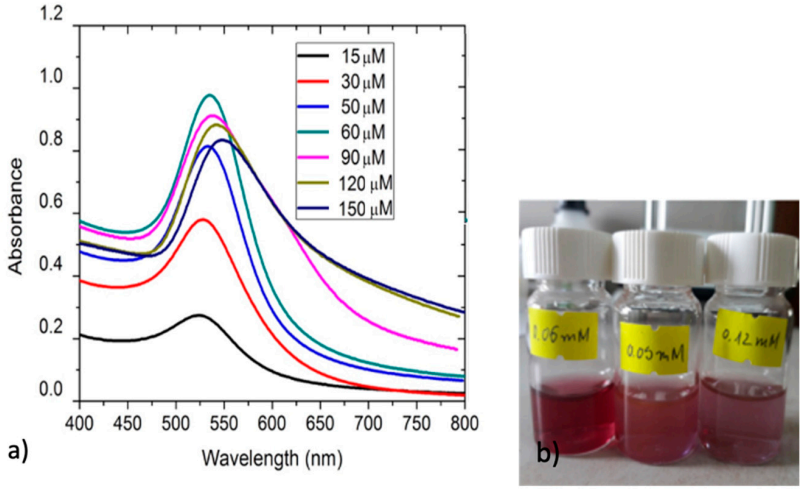

Figure 4. Absorption spectra (**a**) and images (**b**) of the different gold nanoparticle solutions synthesized from different precursor concentrations.

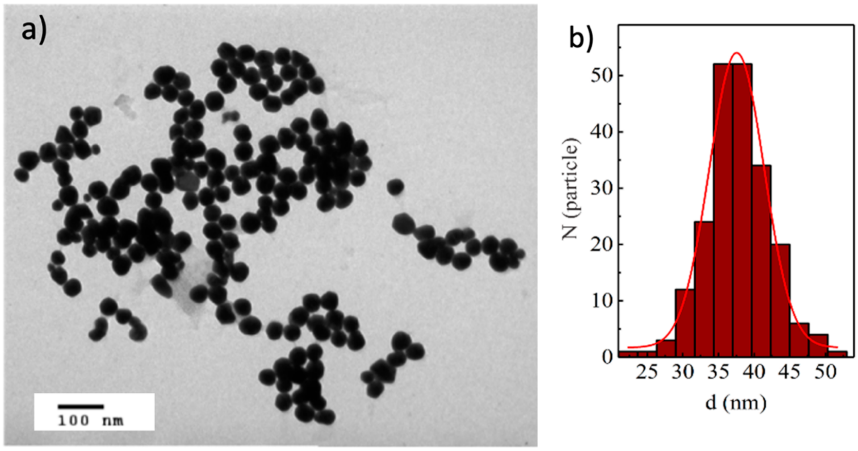

Figure 5. TEM image (**a**) and particle size distribution histogram (**b**) of gold nanoparticles (AuNPs) produced by the plasma–liquid interaction method with a precursor concentration of 0.06 mM.

Figure 6 presents the TEM images of the nontreated Au/TiO_2 nanocomposite. One can easily see that the AuNPs are no longer homogenous and uniform in shape, but their size is distributed in the range from about 10 nm to around 55 nm. This is in line with the broader absorption band in their UV-vis absorption spectra (Figure 7). It is likely that these AuNPs are formed in the solution before being attached to TiO_2 surface because they show similar size distribution as those generated from the pure $HAuCl_4$. All generated AuNPs are seen immobilized on the TiO_2 surface with clear and sharp boundaries indicating a rather weak connection between them. This also supports a small red shift of about 15 nm compared to the situation with the pristine AuNPs. The influence of TiO_2 on the reduction mechanism of Auric ions may be twofold: catalyst effect under UV radiation from plasma which enhances the particle formation, resulting in bigger particles and growth termination by capturing the growing particles onto the titania surface.

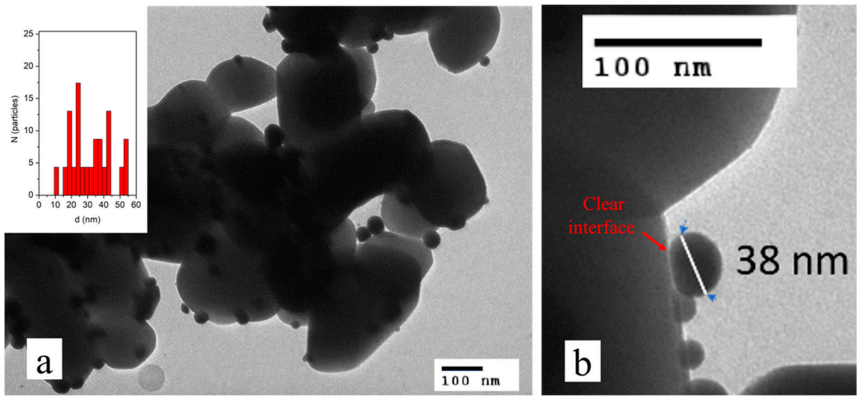

Figure 6. TEM image (**a**) of non-treated Au/TiO_2 nanocomposites produced by the plasma–liquid interaction method with a precursor concentration of 0.06 mM, the inset shows the particle size distribution histogram of gold nanoparticles. Magnification of TEM image (**b**) elucidating the sharp boundary between TiO_2 surface and gold nanoparticle.

Unlike the non-treated Au/TiO_2, there are two types of AuNPs existing in the treated Au/TiO_2, one with a similar size distribution as in the non-treated Au/TiO_2 composites and the other with very small sizes ranging from 4 nm to 9 nm (Figure 8). Both of these types exhibit noticeably close contacts to the TiO_2 surface with seemingly undetectable boundaries. The small particles even seem to be submerged into the TiO_2 matrix (see Figure 8). The UV-vis spectra (Figure 7) of this sample show a good agreement with the TEM results. The spectra of the treated Au/TiO_2 show two absorption peaks which can be attributed to the two classes of AuNP particle size (there is no AuNP aggregation).

The absorption peaks are strongly red shifted from about 523 nm to 538 nm (for smaller AuNPs) and from 534 nm to around 680 nm (for larger AuNPs). Using the refractive index difference of 1.279 (rutile TiO_2 has refractive index of 2.609) applied for the situation presented in Figure 5 in [21], one can easily estimate the red shift for particles with the original plasmonic resonance of 534 nm in water (n = 1.33) to be about 130 nm which is in good agreement with the red shift of the larger sized AuNPs in the treated Au/TiO_2. This result again confirms a strong contact between the treated TiO_2 and the AuNPs in treated Au/TiO_2 nanocomposites.

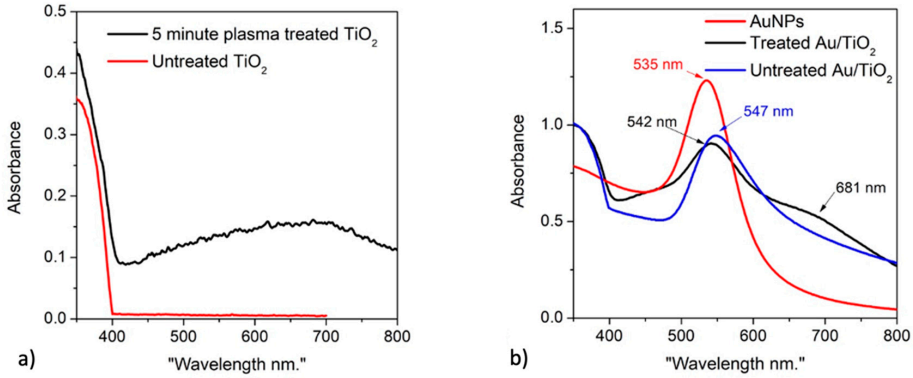

Figure 7. Extinction UV-vis spectra of (**a**) non-treated rutile TiO_2 (red curve), treated rutile TiO_2 with 3% NH_3, 3% H_2O_2 under a 5 min plasma treatment (black curve) and (**b**) bare Au-nanoparticles generated from 0.06 mM $HAuCl_4$ (red curve), non-treated Au/TiO_2 nanocomposite (blue curve), and treated Au/TiO_2 nanocomposite (black curve).

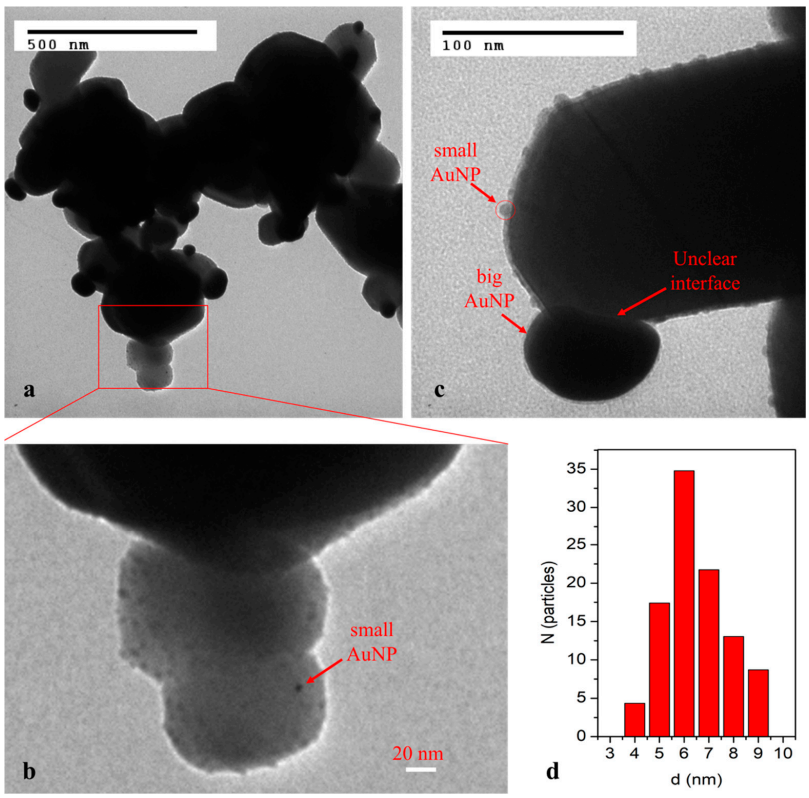

Figure 8. TEM images (**a**) of the treated Au/TiO_2 nanocomposite produced by the plasma–liquid interaction method with the precursor concentration of 0.06 mM. Magnification of TEM images elucidating (**b**) the submerging of small gold nanoparticles into TiO_2 surface and (**c**) the close contact between gold nanoparticle and TiO_2 surface. The particle size distribution histogram (**d**) of small gold nanoparticles of the same sample.

As expected from the above analysis, the MB sunlight degradation rate of the non-treated Au/TiO_2 was improved in comparison to that of bared TiO_2 (Figure 9). Even weakly attached AuNPs already increased the degradation rate by a factor of 4 from 0.01 min^{-1} with TiO_2 to 0.04 min^{-1}, with non-treated Au/TiO_2 supporting the electron–hole separation and absorption spectra broadening. This effect is maximized in the treated Au/TiO_2 as the degradation rate reaches the extremely high value of 0.13 min^{-1}. This value is far better than the MB sunlight degradation rate in the order of only 0.022 min^{-1} obtained with the AuNPs doped TiO_2 prepared by the chemical method, as reported by S. Padikkaparambil et al. [22].

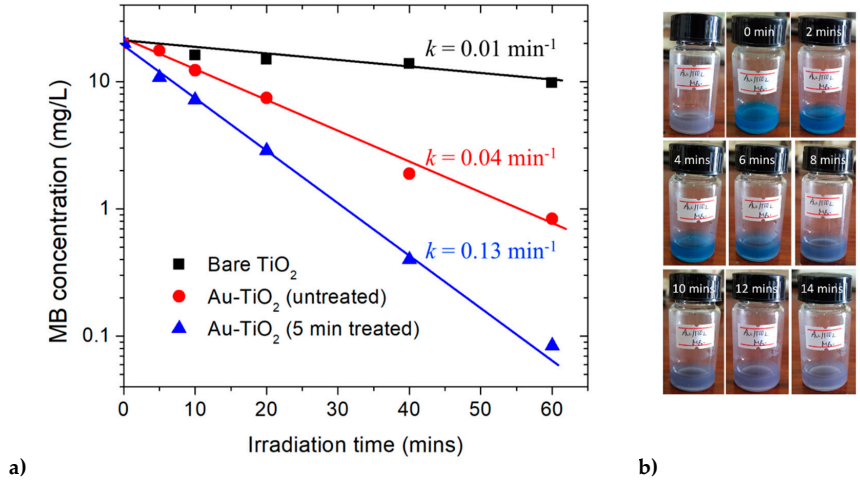

Figure 9. Kinetics of Methylene blue (MB) degradation (**a**) in the presence of bare TiO_2 and Au/TiO_2 nanocomposite in sunlight and decolorization of MB with Au/TiO_2 (5 min plasma treated) under sunlight radiation (**b**).

4. Conclusions

A high performance sunlight photocatalyst of the type Au/TiO_2 nanocomposite has been successfully synthesized by the incorporation of gold nanoparticles (AuNPs) onto the TiO_2 surface using the plasma–liquid interaction method. This method is proven to be efficient and environmentally clean in terms of minimizing processing time and the usage of treating agents. There are two types of AuNPs confined in the treated Au/TiO_2 samples: the small size AuNPs, with the size of about 2 nm, may grow directly on the TiO_2 surface, while the larger size AuNPs with the particle size distributed around about 40 nm grow in the solution before being attached onto the TiO_2 surface.

The plasma enhanced surface activation has brought a potentially strong improvement of the grafting of AuNPs onto the TiO_2 surface. The contact between the AuNPs and TiO_2 in the treated Au/TiO_2 sample is tight which results in a very strong red shift of the plasmonic resonant peak. The sunlight degradation rate of MB with treated Au/TiO_2 has increased 3.25 times in comparison to that of the non-treated Au/TiO_2 and even by the factor of 13 in comparison to that of the bare rutile TiO_2.

Author Contributions: Conceptualization, J.H.K., S.I.K. and D.H.T.; investigation, N.T.T.T., L.H.M. and P.H.M.; writing—original draft preparation, N.T.T.T. and D.H.T.; writing—review and editing, N.T.T.T., N.T.H., J.H.K., S.I.K. and D.H.T.; supervision, D.H.T.; project administration, P.H.M. All authors have read and agreed to the published version of the manuscript.

Funding: This work was financially supported by the International Center of Physics under the auspices of UNESCO and project number QTRU01.01/19-20, and Russian Foundation for Basic Research (grant # 19-52-54003 Viet_a).

Conflicts of Interest: The authors declare no conflict of interest.

References

1. Serpone, N.; Emeline, A.V.; Horikoshi, S.; Kuznetsov, V.; Ryabchuk, V.K. On the genesis of heterogeneous photocatalysis: A brief historical perspective in the period 1910 to the mid-1980s. *Photochem. Photobiol. Sci.* **2012**, *11*, 1121–1150. [CrossRef] [PubMed]
2. Teichner, S.J. The origins of photocatalysis. *J. Porous Mater.* **2007**, *15*, 311–314. [CrossRef]
3. Ozawa, K.; Emori, M.; Yamamoto, S.; Yukawa, R.; Yamamoto, S.; Hobara, R.; Fujikawa, K.; Sakama, H.; Matsuda, I. Electron–Hole Recombination Time at TiO2 Single-Crystal Surfaces: Influence of Surface Band Bending. *J. Phys. Chem. Lett.* **2014**, *5*, 1953–1957. [CrossRef] [PubMed]
4. Valencia, S.; Marín, J.M.; Restrepo, G. Study of the Bandgap of Synthesized Titanium Dioxide Nanoparticules Using the Sol-Gel Method and a Hydrothermal Treatment. *Open Mater. Sci. J.* **2010**, *4*, 9–14. [CrossRef]
5. Linic, S.; Christopher, P.; Ingram, D.B. Plasmonic-metal nanostructures for efficient conversion of solar to chemical energy. *Nat. Mater.* **2011**, *10*, 911–921. [CrossRef]
6. Kochuveedu, S.T.; Jang, Y.H.; Kim, D.H. A study on the mechanism for the interaction of light with noble metal-metal oxide semiconductor nanostructures for various photophysical applications. *Chem. Soc. Rev.* **2013**, *42*, 8467–8493.
7. Chan, S.C.; Barteau, M.A. Preparation of Highly Uniform Ag/TiO2and Au/TiO2Supported Nanoparticle Catalysts by Photodeposition. *Langmuir* **2005**, *21*, 5588–5595. [CrossRef]
8. Damato, T.C.; De Oliveira, C.C.S.; Ando, R.A.; Camargo, P.H.C. A Facile Approach to TiO2 Colloidal Spheres Decorated with Au Nanoparticles Displaying Well-Defined Sizes and Uniform Dispersion. *Langmuir* **2013**, *29*, 1642–1649. [CrossRef]
9. Liu, J.; Zhou, Y.; Han, F.; Chen, D.; Chen, L. Synthesis of mesoporous Au-TiO2 nanocomposites via a one-pot sol-gel process with enhanced photocatalytic activity. *Mater. Lett.* **2017**, *207*, 109–112. [CrossRef]
10. Ninsonti, H.; Sriwichai, S.; Wetchakun, N.; Kangwansupamonkon, W.; Phanichphant, S. Au-loaded TiO2 and Ag-loaded TiO2 synthesized by modified sol–gel/impregnation method as photocatalysts. *Jpn. J. Appl. Phys.* **2015**, *55*, 02BC05. [CrossRef]
11. Rehacek, V.; Hotovy, I.; Vojs, M. Treatment of TiO2 surface for deposition of gold nanoparticles from colloidal suspension. *J. Micromech. Microeng.* **2015**, *25*, 74008. [CrossRef]
12. Higgins, M.C.M.; Clifford, D.; Rojas, J.V. Au@TiO2 nanocomposites synthesized by X-ray radiolysis as potential radiosensitizers. *Appl. Surf. Sci.* **2018**, *427*, 702–710. [CrossRef]
13. Ostrikov, K.; Neyts, E.C.; Meyyappan, M. Plasma nanoscience: From nano-solids in plasmas to nano-plasmas in solids. *Adv. Phys.* **2013**, *62*, 113–224. [CrossRef]
14. Maguire, P.D.; Rutherford, D.; Macias-Montero, M.; Mahony, C.; Kelsey, C.; Tweedie, M.; Pérez-Martin, F.; McQuaid, H.; Diver, D.A.; Mariotti, D. Continuous In-Flight Synthesis for On-Demand Delivery of Ligand-Free Colloidal Gold Nanoparticles. *Nano Lett.* **2017**, *17*, 1336–1343. [CrossRef]
15. Kaushik, N.K.; Kaushik, N.; Linh, N.N.; Ghimire, B.; Pengkit, A.; Sornsakdanuphap, J.; Lee, S.-J.; Choi, E.H. Plasma and Nanomaterials: Fabrication and Biomedical Applications. *Nanomaterials* **2019**, *9*, 98. [CrossRef]
16. Tung, D.H.; Thuong, T.T.; Van Duong, P.; Lien, N.T.H.; Minh, P.H.; Ионин, A.; Levchenko, A.O.; Rudenko, A.A.; Saraeva, I.N.; Ivanova, A.K.; et al. Electrochemical Fabrication of Hybrid Plasmonic-dielectric Nanomaterial Based on Gold-diamond Clusters. *Commun. Phys.* **2017**, *27*, 37. [CrossRef]
17. Myroshnychenko, V.; Rodríguez-Fernández, J.; Pastoriza-Santos, I.; Funston, A.M.; Novo, C.; Mulvaney, P.; Liz-Marzán, L.M.; De Abajo, F.J.G. Modelling the optical response of gold nanoparticles. *Chem. Soc. Rev.* **2008**, *37*, 1792. [CrossRef]
18. Bruggeman, P.J.; Kushner, M.J.; Locke, B.R.; Gardeniers, H.; Graham, W.G.; Graves, D.B.; Hofman-Caris, R.C.H.M.; Maric, D.; Reid, J.P.; Ceriani, E.; et al. Plasma–liquid interactions: A review and roadmap. *Plasma Sources Sci. Technol.* **2016**, *25*, 53002. [CrossRef]
19. Rumbach, P.; Bartels, D.M.; Sankaran, R.M.; Go, D.B. The solvation of electrons by an atmospheric-pressure plasma. *Nat. Commun.* **2015**, *6*, 7248. [CrossRef]
20. Patel, J.; Nemcova, L.; Maguire, P.D.; Graham, W.; Mariotti, D. Synthesis of surfactant-free electrostatically stabilized gold nanoparticles by plasma-induced liquid chemistry. *Nanotechnology* **2013**, *24*, 245604. [CrossRef]

21. Miller, M.M.; Lazarides, A.A. Sensitivity of Metal Nanoparticle Surface Plasmon Resonance to the Dielectric Environment. *J. Phys. Chem. B* **2005**, *109*, 21556–21565. [CrossRef] [PubMed]
22. Padikkaparambil, S.; Narayanan, B.; Yaakob, Z.; Viswanathan, S.; Tasirin, S.M. Au/TiO2 Reusable Photocatalysts for Dye Degradation. *Int. J. Photoenergy* **2013**, *2013*, 752605. [CrossRef]